



Cumulative minor loop growth in Co/Pt and Co/Pd multilayers

A. Berger,¹ S. Mangin,² J. McCord,³ O. Hellwig,⁴ and E. E. Fullerton⁵

¹*CIC nanoGUNE Consolider, E-20018 Donostia - San Sebastián, Spain*

²*IJL, Nancy-Université, CNRS UMR 7198, F-54506 Vandoeuvre Cedex, France*

³*Institute of Ion Beam Physics and Materials Research, Forschungszentrum Dresden-Rossendorf, D-01328 Dresden, Germany*

⁴*San Jose Research Center, Hitachi Global Storage Technologies, San Jose, California 95135, USA*

⁵*Center for Magnetic Recording Research, University of California, La Jolla, California 92093-0401, USA*

(Received 7 May 2010; published 20 September 2010)

The behavior of minor hysteresis loops in perpendicular anisotropy [Co/Pt] and [Co/Pd] multilayers has been investigated. Upon applying a succession of identical magnetic field cycles, we observe a very substantial cumulative growth of the minor loop area. For the [Co/Pt] multilayers this effect only saturates near complete magnetization reversal while the behavior is slightly more limited for [Co/Pd] multilayers. We also find this cumulative growth to occur even if the minor loop field cycles are made asymmetric by means of a positive bias field. The cumulative behavior persists up to a sample-dependent threshold value above which this effect disappears. In all samples, the cumulative minor loop growth is correlated with a small reduction in the maximum magnetization value in each cycle. Magneto-optical Kerr microscopy studies correlate the minor loop growth with the memory and cumulative expansion of lateral domain cycling. All experimental observations can be consistently explained as an accumulation of small nucleation domains that aid subsequent reversals and facilitate the cumulative minor loop growth.

DOI: [10.1103/PhysRevB.82.104423](https://doi.org/10.1103/PhysRevB.82.104423)

PACS number(s): 75.60.Jk, 75.70.Cn

I. INTRODUCTION

A key aspect of ferromagnetic materials is the occurrence of hysteresis, which is generally observed as a branching of the magnetization M vs external field H dependency.¹ Fundamentally, this nonequilibrium phenomenon is the result of a first-order phase transition occurring upon reversal of the external magnetic field H . In the vicinity of this reversal, the magnetic free energy exhibits more than one stable or metastable state, making the state occupied by a ferromagnet dependent on the field history.¹ $M(H)$ becomes a single-valued function only for fields large enough to suppress the population of all metastable states in the time frame of the measurement. The minimum field, at which such a single-valued relation is reached, is the closure field H^* .² Thus, hysteresis loops measured with a maximum applied field $H_{\max} > H^*$ have well-defined starting points and are referred to as the major loop whereas loops with $H_{\max} < H^*$ are called minor loops.¹

While it is well established that hysteresis loops show a pronounced temperature and frequency dependence, it is generally assumed that a ferromagnetic sample produces a unique hysteresis loop under identical external conditions.^{3,4} This perceived uniqueness allows the utilization of hysteresis loop measurements as a material characterization method and is furthermore important in applications. Indeed, ferromagnetic materials are most frequently utilized according to their specific hysteresis properties.⁵ However, magnetization reversal is a stochastic process at nonvanishing temperatures, and therefore typically progressing along multiple microscopic pathways.⁶ This particular aspect was highlighted by a number of recent experimental studies in which the absence of microscopic repeatability was found for major hysteresis loops in several material systems.^{7–10} Nonetheless, M vs H loops are, in general, an accurate characterization tool for

macroscopic samples because the volume averaged magnetization $\langle M \rangle$ repeats itself with a very high degree of accuracy due to statistical averaging and the fact that all reversal processes are driven toward lowering the Zeeman energy, which is proportional to $\langle M \rangle$.¹¹

The above statements about the repeatability of hysteresis loops have to be differentiated between major and minor loops. While the macroscopic $M(H)$ curve is generally unique for major loops, the absence of $M(H)$ repeatability is more commonly found in minor loops if they are measured consecutively, even though changes are typically small.¹² Most commonly, minor loops show a small driftlike motion without a substantial change in shape or size, which is generally referred to as accommodation or reptation. These effects are especially visible if the applied minor loop field sequence $H(t)$ is biased, i.e., has a time-averaged net value $\langle H \rangle \neq 0$.^{13,14} In addition to such driftlike minor loop changes, Ferre *et al.*¹⁵ observed also a modest increase in between repeated minor loops for ultrathin Co/Au films. In general, the repeatability of minor loops is an important materials property, because magnets are exposed to field cycles with $H < H^*$ in many applications and, more fundamentally, because numerous hysteresis models and characterization techniques are based on the assumption of stable minor loops.^{16–22}

In this paper, we describe a cumulative growth effect in the time-evolution $M(t)$ upon applying a cyclical magnetic field $H(t)$ for Co/Pt and Co/Pd multilayers with perpendicular anisotropy. The effect leads to a substantial growth of the minor loop area upon field cycling and differs from the more commonly reported driftlike behavior.^{13,14} As mentioned above, Ferré *et al.*¹⁵ also observed a growth of minor loops upon multiple cycling but the effect was rather modest in comparison to our findings and occurred only in a very narrow field range. Furthermore, no other details, such as its

field dependence, for instance, were reported. Other aspects of unusual magnetization reversal behavior were recently reported for Co/Pt multilayers by Iudin *et al.*²³ They observed not only asymmetric domain nucleation in their samples but also time-dependent effects that are consistent with asymmetric domain expansion and retraction dynamics in minor loops. However, no specific study of multiloop behavior and its applied field dependence was presented. Asymmetric domain-wall dynamics was also observed in lithographically defined magnetic microstructures that were specifically designed for this purpose to facilitate a magnetic domain-wall ratchet.²⁴

The specific multilayer structures, used in our study, are $[\text{Co}(4 \text{ \AA})/\text{Pt}(7 \text{ \AA})]_X$ and $[\text{Co}(4 \text{ \AA})/\text{Pd}(7 \text{ \AA})]_X$ with $5 < X < 10$. The samples were deposited by magnetron sputtering (3 mT Ar pressure) onto ambient temperature Si-nitride coated Si substrates. As seed layers, we used 200 \AA Pt for the Co/Pt multilayers as well as a 30 \AA Pd underlayer for the Co/Pd multilayers. These deposition conditions produce magnetic multilayers with an easy axis along the surface normal and large enough anisotropies to produce high remanent magnetization. X-ray diffraction measurements confirmed a (111) crystalline texture for both types of multilayers. Hysteresis loop studies were performed by using an alternating gradient magnetometer as well as a superconducting quantum interference device (SQUID) magnetometer, and laterally resolved studies were done using a magneto-optical Kerr effect microscope equipped with an air coil for the application of perpendicular fields. For all the measurements presented here the field was applied perpendicular to film plane, i.e., along the anisotropy axis.

II. Co/Pt MULTILAYER RESULTS

Fig. 1 shows an example of the $M(H)$ dependence for a $[\text{Co}(4 \text{ \AA})/\text{Pt}(7 \text{ \AA})]_8$ -multilayer film upon cycling an external field $H < H^*$ multiple times in comparison with the major hysteresis loop measured for the same sweep rate. The inset of Fig. 1 is a schematic of the H vs time t sequence used in this experiment, for which a period of $T=80$ s was used. The $H(t)$ sequence was chosen to be symmetric around $H=0$ with a maximum and a minimum applied field such that $H_{\max} = -H_{\min} = 290$ Oe, which is about 10% smaller than the coercivity for this sample. Prior to the actual measurement sequence, a sufficiently high field $H_0 = 1$ kOe $> H^*$ was applied to start the measurement sequence in a well-defined magnetic state.²⁵ As one can see from Fig. 1, the resulting minor loops show neither repeatability nor a driftlike dependence. Instead, the loops show a very pronounced asymmetric growth. While the upper part of the magnetization curves appears to fall back onto the major loop in each cycle, the lower part reaches increasingly lower magnetization levels. The amount of magnetization reversal ΔM , defined as

$$\Delta M = \frac{1}{2} \frac{(M_{\max} - M_{\min})}{M_S} \quad (1)$$

is cumulative, i.e., increasing with each successive minor loop cycle. Hereby, M_{\max} and M_{\min} are the maximum and minimum magnetization values in each cycle, respectively. It

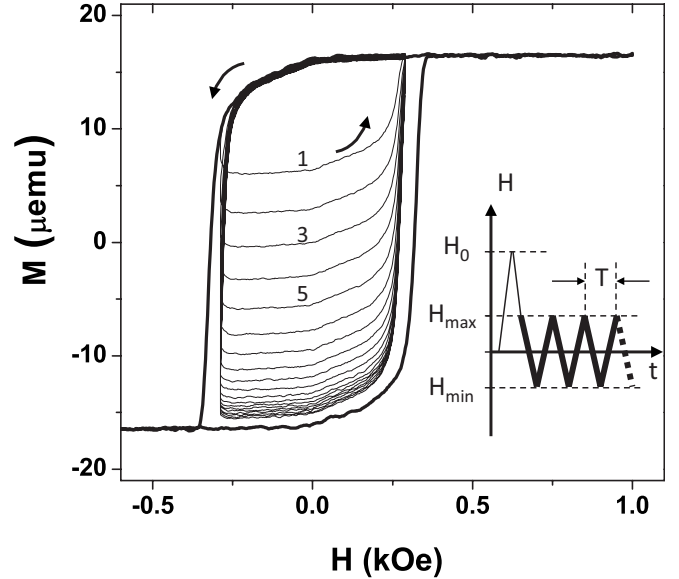


FIG. 1. Field dependence of the magnetization for a $(\text{Co}/\text{Pt})_8$ multilayer. The thick solid line represents the major loop behavior while the thin solid line shows a sequence of successive minor loops upon applying a symmetric field amplitude of $H_{\max} = -H_{\min} = 290$ Oe. The first, third, and fifth minor loop are labeled. The inset is a schematic of the H vs t dependence, which was applied for this measurement.

is noteworthy that the effect is large, changing ΔM from about 25% of the saturation magnetization M_S for the first minor loop to nearly 90% of M_S for the 19th minor loop repetition, increasing the hysteresis loss of the minor loops to about 350% of its original value in this sample.

To follow the time evolution of such multiple minor loops in more detail, we have plotted M vs t directly in Fig. 2(a) for several experiments using different field amplitudes H_{\max} . From these curves we can make the following observations: (i) all curves show clearly an increase in the magnetization reversal amplitude upon field cycling, making it evident that the cumulative hysteresis loop growth is a general phenomenon in our samples; (ii) the data for $H_{\max} = 300$ Oe indicate that this growth only stops once full or nearly full magnetization reversal is achieved; and (iii) the number of cycles needed to reach full magnetization reversal increases for decreasing field amplitude. The envelope function for all curves follows an exponential saturation behavior. Therefore, we have analyzed the measured $M(t)$ curves by performing least-squares fits of

$$M(t) = M_S \cdot \left\{ 1 - \left[1 - \exp\left(-\frac{t_1}{\tau}\right) \right] \cdot (\sin(t_2) + 1) \right\} \quad (2)$$

$$\text{with } t_i = t + \varphi_i \quad (3)$$

to all data sets. Here, τ is the time constant for approaching full magnetization reversal and the φ_i are time phase factors for the envelope function and the oscillatory term of Eq. (2), respectively. The solid lines in Fig. 2(a) represent the results of these fits. The envelope function is very well reproduced, indicating that these minor loop oscillations approach full

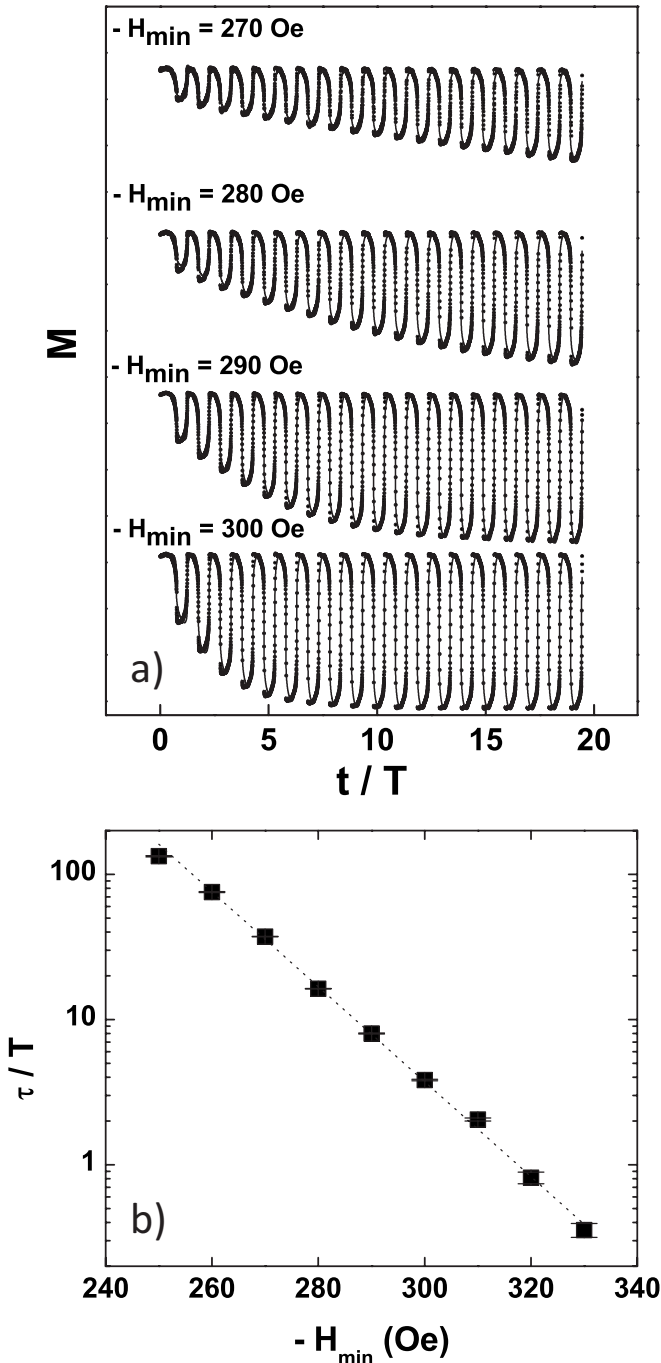


FIG. 2. (a) $M(t)$ dependence for successive minor loop cycles measured for a $(\text{Co/Pt})_8$ multilayer. The different curves were measured for different peak values of the magnetic field H_{max} ($=-H_{\text{min}}$). The time is given in units of the cycle period $T=80$ s, which was held constant for all experiments. The experimental data are shown as (\bullet) while the solid lines represent least-squares fits of Eq. (2); (b) relaxation time constant τ , derived from the least-squares fits of Eq. (2) to the experimental data, as a function of $-H_{\text{min}}$. The squares are the results of the individual fits while the dashed line illustrates exponential field dependence according to Eq. (4).

magnetization reversal with a characteristic τ , which is strongly dependent on the applied field amplitude H_{max} . Figure 2(b) shows the values of the time constant τ , given in

units of the oscillation period T , as a function of H_{max} in a semilogarithmic plot. As one can see from these data, τ increases strongly with decreasing field amplitude and follows very closely an inverse exponential behavior,

$$\tau \sim \exp\left(-\frac{H}{H_0}\right), \quad (4)$$

which is indicated by the dashed line in Fig. 2(b). H_0 is a sample-dependent constant. Such a behavior is consistent with a thermally activated process, in which the activation barrier of the controlling reversal mechanism is linearly dependent on the externally applied field. While such a characteristic is typically indicative of domain-wall motion by means of thermally activated depinning,^{15,26} it is unusual here that the process is very asymmetric, i.e., completely different on the reversal starting side near H_{min} and the loop completion side at H_{max} . While the magnetization appears to return to full positive M_S at H_{max} , the reversal amplitude ΔM increases with every successive reversal. This finding is, however, consistent with other observations for this class of materials, i.e., ultrathin films and multilayers with perpendicular magnetic anisotropy. As reported in the work by Ferre *et al.*¹⁵ as well as in some very recent works on Co/Pt multilayers²⁷ and CoB thin films,²⁸ such films exhibit asymmetric remagnetization processes, meaning that it is easier to magnetize them back to the original state by inverting the magnetic field than to completely reverse the magnetization by keeping the field applied. In these studies, it is also observed that it is even easier to invert the magnetization process than initially start the magnetization reversal process.^{15,27,28}

Despite this minor loop asymmetry and the ease with which remagnetization occurs, our Co/Pt samples exhibit a multiloop memory, so that they cannot really return to full positive magnetization or identical magnetization states at H_{max} upon successive field cycling. Instead, the system must

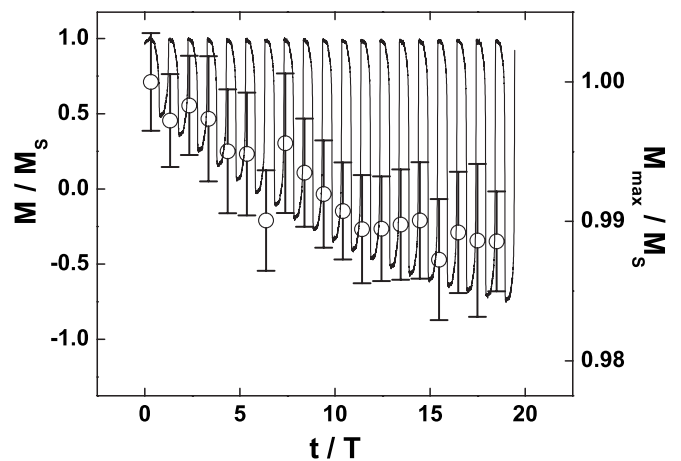


FIG. 3. $M(t)$ dependence for successive minor loop cycles measured for a $(\text{Co/Pt})_8$ multilayer. The solid line, corresponding to the left-hand scale, shows the complete time evolution upon applying a field sequence with $H_{\text{max}}=-H_{\text{min}}=280$ Oe. The open circles (\circ) show the maximum magnetization M_{max} reached in every cycle and correspond to the right-hand scale.

“remember” the previous cycles in a way that produces only very small deviations from saturation. This behavior can indeed be observed in Fig. 3, in which $M(t)$ is compared with M_{\max} , i.e., the maximum magnetization reached in every minor loop. As one can see from the comparison, M_{\max} exhibits a very small decline upon multiple cycling of the field, barely above the noise level of the experiment. While M_{\max} only declines by about 1%, ΔM reaches more than 85% of M_S , thus masking the M_{\max} decline. Figure 3 furthermore indicates that the M_{\max} decline is synchronous with the ΔM increase because $M_{\max}(t)$ follows the envelope function of $M(t)$ and is characterized by the same τ . Our results therefore show that while initial remagnetization processes upon field reversal require lower fields, just as previously reported,^{15,27,28} the same is not true near saturation, where it becomes increasingly more difficult to reach the same magnetization value with every minor loop cycle.

III. Co/Pd-MULTILAYER RESULTS

Figure 4(a) shows the magnetization reversal amplitude ΔM as a function of time for different oscillation fields $H_{\max} = -H_{\min}$, i.e., symmetric minor loops, for a $[\text{Co}(4 \text{ \AA})/\text{Pd}(7 \text{ \AA})]_8$ multilayer sample. Also here, we observe a substantial cumulative increase in the minor loop amplitude and hysteresis loop area for successive field cycles. Furthermore, we find that the time constant, with which a stable minor loop is reached, decreases with increasing field amplitude, just as in the case of the previously shown Co/Pt multilayers. This is visible in Fig. 4(b), where the relaxation time constant τ is displayed as a function of the field amplitude H_{\max} . Also here we see the exponential field dependence of the relaxation time, indicated by the straight line in the semilogarithmic plot.

There is, however, one obvious difference in between the Co/Pd- and the Co/Pt-multilayer samples we investigated. As one can see from the data in Fig. 4(a) and the corresponding data fits for the magnetization reversal amplitude ΔM , the limiting amplitude of the minor loop oscillation is not the same for all applied fields and it also is clearly smaller than the full saturation magnetization for the Co/Pd case, whereas the assumption of M_S as the limiting oscillation amplitude independent from the field, i.e., Eq. (2), worked well for the Co/Pt case. Correspondingly, Eq. (2) is not suitably to describe the observed behavior here and has to be modified. Also, the number of $M(t)$ -data points per minor loop cycle in our Co/Pd measurement was much more limited due to the fact that these measurements were done by means of a SQUID magnetometer and we tried to keep the cycle time T comparable to the Co/Pt-multilayer case. Thus, we directly fit the minor loop amplitude ΔM as a function of time, just as shown in Fig. 4(a). For this, we then utilized

$$\Delta M(t) = \Delta M_{\max} \cdot \left[1 - \exp\left(-\frac{t}{\tau}\right) \right] \quad (5)$$

to determine the time constant values τ displayed in Fig. 4(b). But despite these technical differences and the somewhat more limited growth of the minor loops in these Co/Pd samples, the basic observations of cumulative growth, expo-

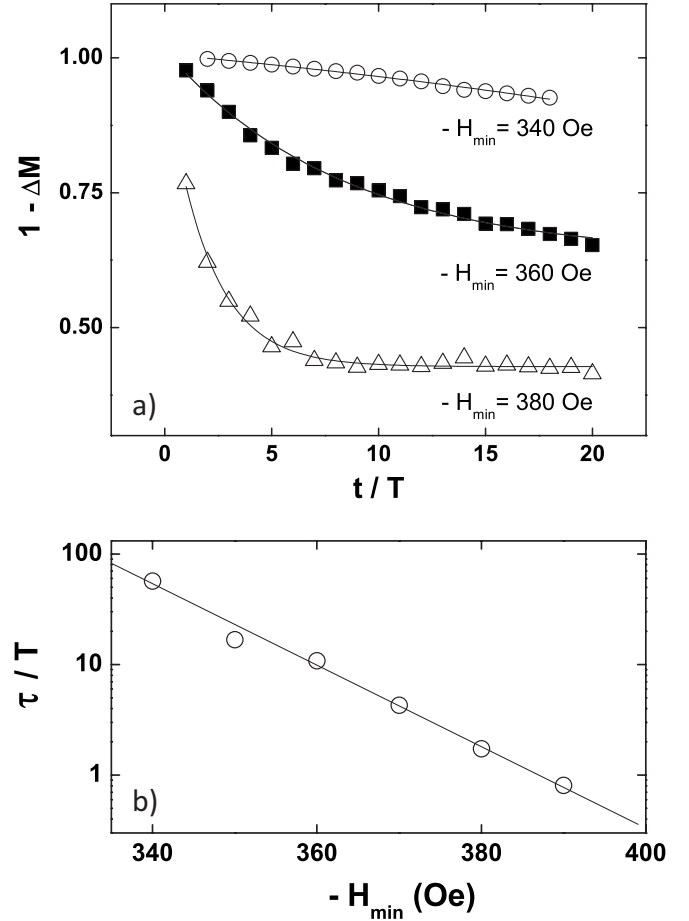


FIG. 4. (a) $\Delta M(t)$ dependence for successive minor loop cycles measured for a $(\text{Co}/\text{Pd})_8$ multilayer upon applying symmetric field sequences of varying strength $H_{\max} = -H_{\min}$; (b) relaxation time constant τ , derived from the least-squares fits of Eq. (5) to the experimental data, as a function of $-H_{\min}$. The circles are the results of the individual fits while the line illustrates exponential field dependence according to Eq. (4).

nential saturation approach, and an exponential field dependence of the relevant time constant are identical in both material systems.

For the Co/Pd multilayers, we also studied the degree in which the cumulative minor loop growth would be preserved upon applying a positive field bias during the minor loop field cycles. Correspondingly, we performed experiments, in which $H_{\max} > -H_{\min}$. Some of our results are shown in Fig. 5. Figure 5(a) shows a sequence of measurements, in which $H_{\max} = 450$ Oe was held constant, while H_{\min} was varied in the same range as previously used for symmetric magnetic field cycles, shown in Fig. 4. We can see that the cumulative growth behavior is not substantially changed and that the minor loops continue to grow, even though a positive magnetic field far larger than the coercive field is applied as part of the magnetic field cycles. Also the dependence from the minimum field in every cycle is not changed in so far as larger $|H_{\min}|$ values produce faster minor loop growth toward larger saturation values of ΔM , indicating that the here observed processes are fairly independent from H_{\max} . This rather weak dependence on the positive bias field becomes

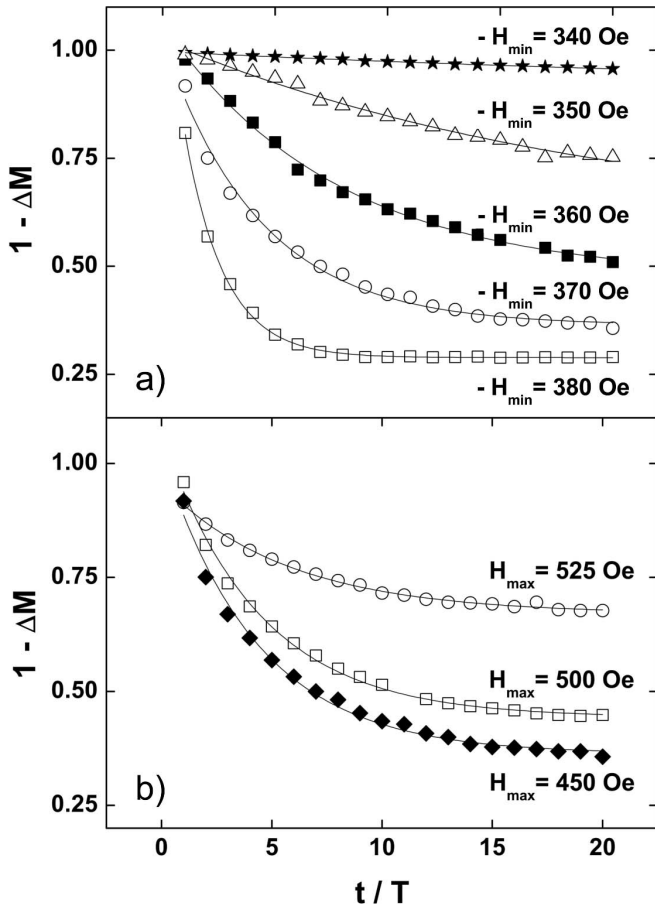


FIG. 5. $\Delta M(t)$ dependence for successive minor loop cycles measured for a $(\text{Co/Pd})_8$ multilayer upon applying asymmetric field sequences: (a) $H_{\text{max}}=450$ Oe for different values of H_{min} ; (b) $-H_{\text{min}}=370$ Oe for different values of H_{max} .

even more evident in Fig. 5(b), where a sequence of measurements is displayed, in which $-H_{\text{min}}=370$ Oe was held constant, while H_{max} was varied in between 450–525 Oe. While there clearly is a dependence on H_{max} , it is however weak, much weaker than the field dependence on H_{min} . Whereas, the 10 Oe steps of H_{min} in Fig. 5(a) cause substantial changes in between the different cumulative growth curves, rather small changes occur for the 25 and 50 Oe steps in H_{max} shown in Fig. 5(b).

This rather weak sensitivity of the cumulative growth on the applied maximum field H_{max} during the minor loop cycle is also observed in the relaxation time constant τ . Figure 6(a) shows the dependence of τ from the applied minimum field H_{min} , just as Figs. 2(b) and 4(b), but for asymmetric field loops with $H_{\text{max}} > -H_{\text{min}}$. We find the relaxation time constants τ to be independent of the applied maximum field H_{max} , at least in the range shown here. So, while the absolute scale of ΔM is moderately changed by increasing H_{max} from 400 to 500 Oe, the corresponding time constant of the cumulative growth is not affected at all. It is only, and very strongly dependent on the minimum field in each cycle H_{min} .

Our Co/Pd-multilayer measurements also corroborate the observed synchronous nature of the M_{max} reduction in every minor loop cycle with the increase in this cycle's amplitude

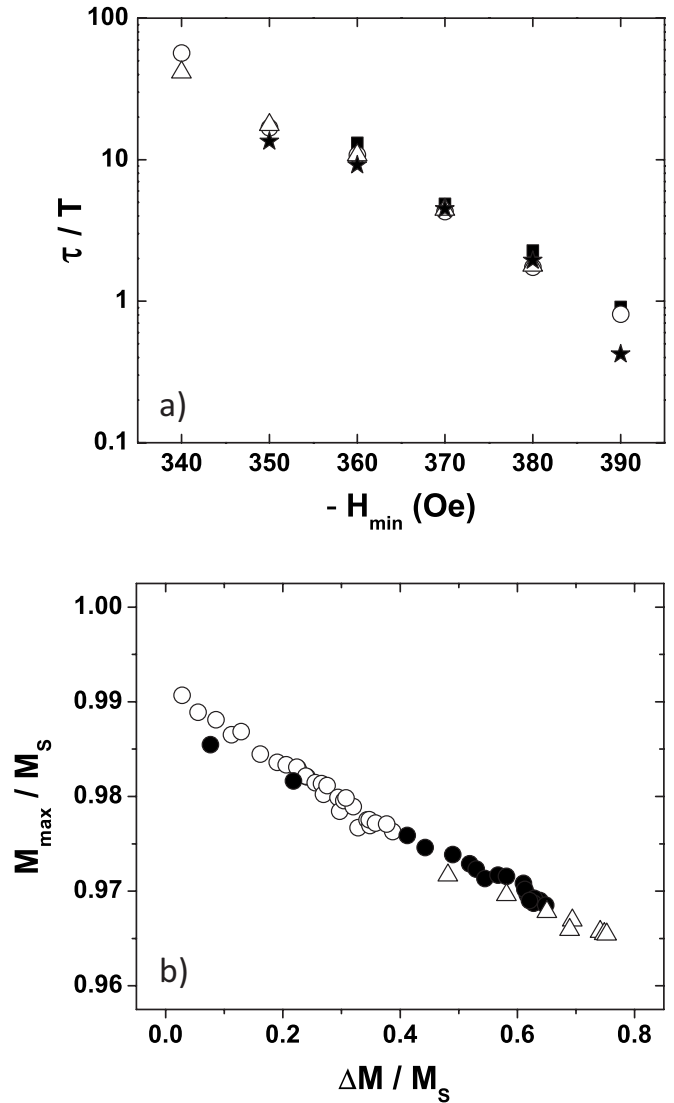


FIG. 6. (a) Relaxation time constant τ , derived from the least-squares fits of Eq. (5) to experimental data from a $(\text{Co/Pd})_8$ multilayer, as a function of $-H_{\text{min}}$ for different values of H_{max} = 500 Oe (■), 450 Oe (○), 400 Oe (△), and $H_{\text{max}}=-H_{\text{min}}$ (★); (b) M_{max} vs ΔM data for successive minor loop cycles with $-H_{\text{min}}=360$ Oe (○), 370 Oe (●), and 380 Oe (△) and fixed $H_{\text{max}}=500$ Oe.

that was shown for the Co/Pt samples in Fig. 3. Figure 6(b) shows M_{max} as a function of ΔM for data measured on a Co/Pd multilayer at various $-H_{\text{min}}$ values with H_{max} held constant at 500 Oe. Here, the M_{max} level and ΔM are fully correlated and show an approximately linear relation. Thus, the change in between multiple minor loops is evident for both quantities, M_{max} and ΔM , but with strongly different amplitudes, yielding a strongly asymmetric expansion of successive minor loops.

Another way to interpret the linear functional relationship in between the M_{max} and ΔM is that if the system is brought back to the same level of M_{max} in every cycle, no further increase in ΔM will occur. Therefore, the only weak dependency of the cumulative growth behavior from the positive bias field H_{max} has to reach a threshold value above which

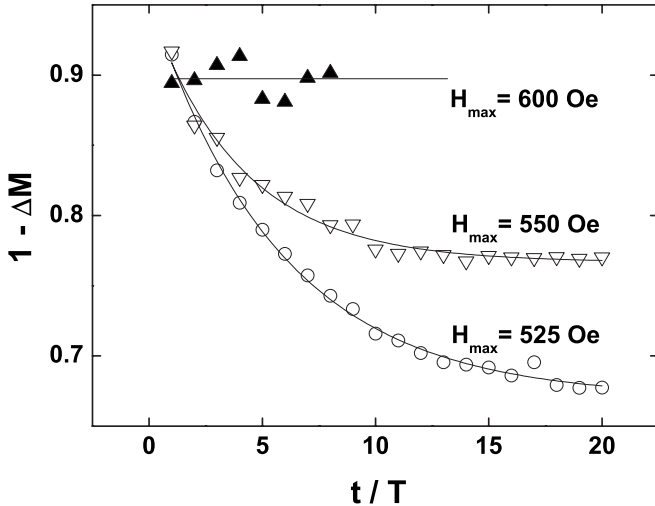


FIG. 7. $\Delta M(t)$ dependence for successive minor loop cycles measured for a $(\text{Co/Pd})_8$ multilayer upon applying asymmetric field sequences for different values of H_{max} and $-H_{\text{min}}=370$ Oe.

the phenomenon has to disappear because M_{max} returns to a stable value even after only one cycle. Apparently the closure field H^* , which we discussed in the introduction would be sufficient to achieve this suppression of the cumulative minor loop growth behavior. Figure 7 shows $\Delta M(t)$ data in this regime. The measurements were done under identical conditions as the ones shown in Fig. 5(b), with the one difference that H_{max} was set higher, up to 600 Oe for this particular Co/Pd sample. We see that while a cumulative minor loop growth is still clearly visible at $H_{\text{max}}=550$ Oe, a field of $H_{\text{max}}=600$ Oe completely suppresses this phenomenon. In this field regime, minor loops are found to be completely stable.

IV. DISCUSSION OF RESULTS

To develop a physical picture and fundamental understanding of the processes associated with the observed macroscopic phenomenon of cumulative minor loop growth, it is important to have an understanding of the microscopic magnetic processes that occur. For this purpose, we have performed magneto-optical microscopy studies on Co/Pd-multilayer samples during subsequent minor hysteresis loop cycles. The applied field values and rate of field change are consistent with our macroscopic measurements. Figure 8 shows a sequence of domain images that are characteristic for the behavior we have found. Every row shows three pictures that were all measured during the same minor loop cycle, and the four rows are pictures taken for four subsequent identical field cycles. The first column (a1)–(d1), shows domain structures at the negative remanent state, meaning they are taken for $H=0$ Oe directly after having been exposed to the maximum negative field of $H_{\text{min}}=-380$ Oe. As one can see from this sequence the sample exhibits a cycle-to-cycle growth of the dark domains that have negative magnetization, i.e., the pictures display cumulative growth in full agreement with our magnetometry data. Furthermore, the strong correlation of the domain structure

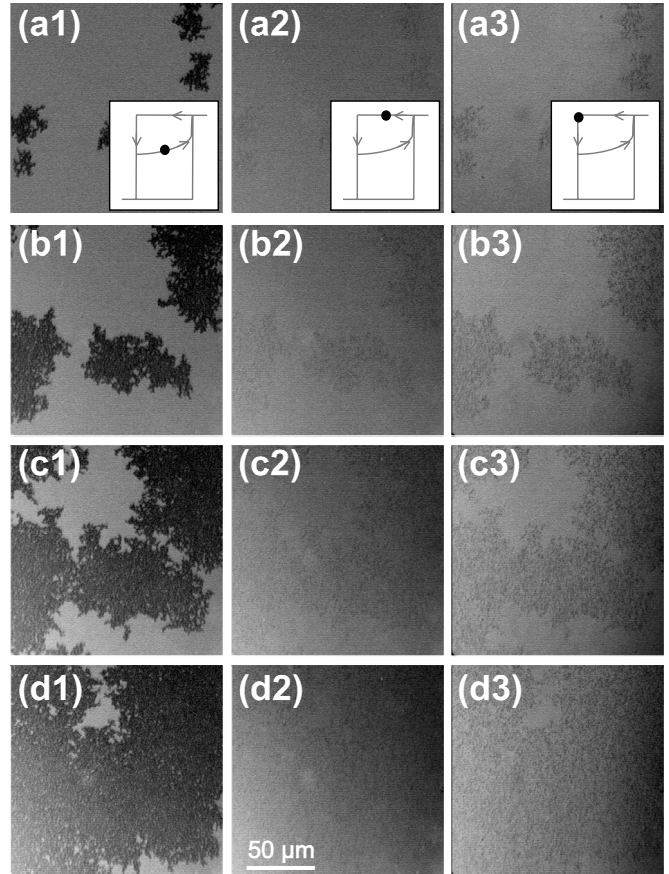


FIG. 8. Sequence of Kerr-effect microscopy images taken on a $(\text{Co/Pd})_8$ -multilayer sample at different points of an asymmetric field sequence ($H_{\text{max}}=500$ Oe, $-H_{\text{min}}=380$ Oe) during consecutive cycles. Columns 1, 2, and 3 correspond to the negative remanent state, the positive remanent state, and the initial negative reversal state at $H=-240$ Oe, respectively. Rows (a)–(d) show pictures taken in four subsequent minor loop cycles. The schematic insets in (a1)–(a3) indicate at which point on the minor loop cycle the observation was made.

that is visible in between the pictures in this column, seems to indicate that the cumulative minor loop growth proceeds by domain expansion, a process that one would expect for a single magnetization reversal in such samples, but not necessarily for multiloop processes.

The middle column of Fig. 8, i.e., pictures (a2)–(d2) show microscopy images of the same location that are taken for $H=0$ Oe directly after having been exposed to the maximum positive field in the minor loop cycle $H_{\text{max}}=500$ Oe and following the acquisition of the first column of pictures. The contrast level for all 12 pictures shown in this figure is identical. Even though some faint contrast may still be visible, the pictures fundamentally show a very uniform magnetization state that appears to be very close to positive saturation, just as we observed macroscopically under those experimental conditions. The right column of pictures in Fig. 8, i.e., (a3)–(d3), shows Kerr microscopy pictures of the same position, measured after the positive remanent pictures were taken and while a negative field of $H=-240$ Oe is being applied. This specific field value, which is reached during the

measurement sequence before the sample is being exposed to H_{\min} , was chosen because it is still above the threshold field strength, at which substantial magnetization reversal sets in. Correspondingly, these pictures show the very initial part of the minor loop reversal after being nearly saturated by the previously applied positive field. In all these pictures, (a3)–(d3), one can see a faint contrast of the initial reversal domains. Furthermore, the lateral pattern appears to be nearly a replica of the previously recorded negative remanent state (left column) in all cases, as far as sufficient details can be recognized above the noise level. This shows, that subsequent negative reversal segments of the minor loop proceed by: (i) first recreating the domain reversal structure that was generated during the previous negative field application, or a domain structure very similar to it, and (ii) second expand the lateral extend of this reversal domain structure, before the magnetic field is increased again, as shown by moving from row to row in Fig. 8. For example, by going from (b3) to (c1), which are successive Kerr images in the overall field sequence, one can see the lateral growth of the reversed (dark) domain structure.

Given the strong perpendicular anisotropy of the multilayered samples that we used for our study, the very substantial contrast difference in between the left and the right column images of Fig. 8 cannot be explained by a different degree of local perpendicular magnetization orientation, i.e., having fully out-of-plane domains in the left column and mostly in-plane oriented domains in the right hand column. Instead the contrast difference must stem from the resolution limit of our Kerr microscope, which may be almost one order below the typical lateral size of perpendicular stripe domains in such multilayer materials.²⁹ Correspondingly, the local contrast that we observe represents the local population balance between up and down domains, in terms of domain size and number. Thus, the faint contrast on the right-hand column means that there are fewer and/or smaller reverse domains present in the same region than there were originally in the preceding negative remanent state, i.e., prior to applying the positive field of 500 Oe.

The local reemergence of previously observed reversal domain pattern at smaller reverse fields than in previous minor cycles, i.e., the behavior seen here in Fig. 8, also requires that the process does not start anew with every new cycle, but instead starts from a preconfigured system, which keeps the reversal domain structure locally memorized. This means that upon applying the positive field a local domain pattern persists that is not completely erased, from which the next cycle of magnetization reversal can expand upon. This behavior is schematically indicated in Fig. 9, which shows a magnetization state sequence similar to the Kerr microscope picture sequence. As one progresses from the negative remanent state (left column) to the positive remanent state in the same minor loop cycle upon applying H_{\max} (middle column), the domain structure breaks up into many small local domains that are preserved, because $H_{\max} < H^*$ is not large enough to annihilate all of them. Such left-over domains have actually been observed by Davies *et al.*³⁰ in thicker Co/Pt-multilayer samples, where they cause anomalies in the hysteresis loops. Also Cheng *et al.*³¹ found channellike substructures in magnetic domains on Co/Pt multilayers, to

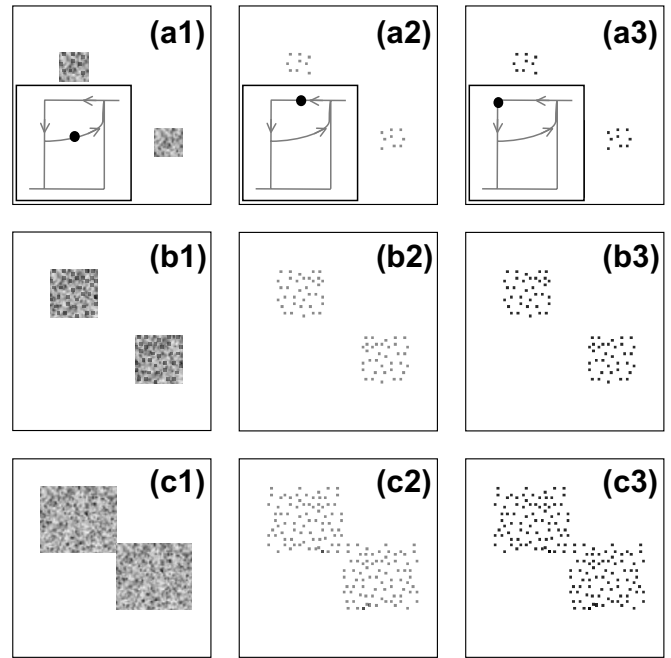


FIG. 9. Schematic of the underlying physical process: the sequence of images shows the domain evolution during consecutive minor loop cycles. Columns 1, 2, and 3 correspond to the negative remanent state, the positive remanent state, and the initial negative reversal state for $H > H_{\min}$, respectively. Rows (a)–(c) illustrate the behavior of three subsequent minor loop cycles. The schematic insets in (a1)–(a3) indicate, which point on the minor loop cycle is represented in every column.

which they attributed unusual magnetization reversal properties such as the field-induced fading of magnetic domains. In experiments like our Kerr microscopy measurements, these leftover domains may not be visible because they are so small that they cannot be resolved and there are so few of them that their signal contribution is insufficient to detect them above the experimental noise, which appears to be the case for the pictures shown in the middle column of Fig. 8. However, they are present as corroborated by our macroscopic measurements of the M_{\max} reduction with every cycle, shown in Figs. 3 and 6(b). This is schematically shown in the center column of Fig. 9 by making the left-over domains visible but with substantially reduced contrast. The right column of Fig. 9 shows the subsequent start of the next negative magnetization reversal cycle by enhancing the local domain contrast through domain growth below the resolution limit of the imaging technique. The larger domain pattern reemerges, just as we have seen in our Kerr microscope images. Here, the left-over domains of the previous cycle now act as the nucleation centers during the next magnetization reversal loop. The overall effect of this sample behavior is that a sequence of reversed minor loop states, such as the ones shown in the left column of Figs. 8 and 9, progresses in a way that resembles simple domain expansion by means of domain-wall movement. In a certain sense, the complete minor loop has no effect but to put a temporary stop on this expansion, even though almost full positive saturation is reached during the minor loop cycle.

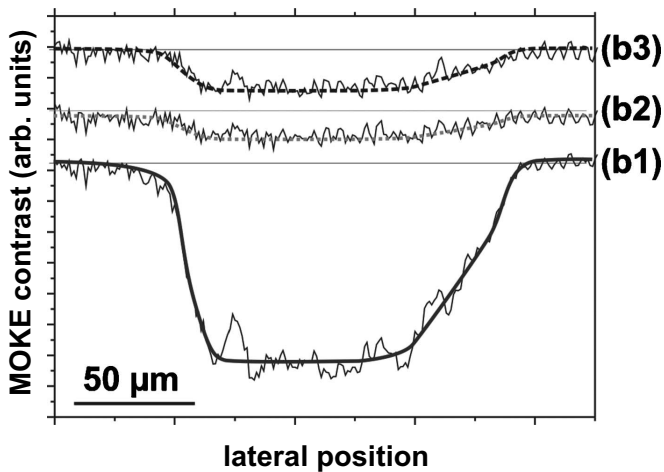


FIG. 10. Sequence of Kerr-effect microscopy line scans taken on a $(\text{Co/Pd})_8$ -multilayer sample at different points of an asymmetric field sequence ($H_{\text{max}}=500$ Oe, $-H_{\text{min}}=380$ Oe) during the same cycle: (b1) \rightarrow (b2) \rightarrow (b3) as shown in Fig. 8.

The here discussed physical picture is furthermore corroborated by the data shown in Fig. 10. Here we see three line scans extracted at the same position from the Kerr images (b1)–(b3) of Fig. 8. Due to the averaging over multiple line scans, we see that not only the near reversal state (b3) shows a clear resemblance to the previous negative remanent state (b1), but also the intermediate remanent state after the positive field H_{max} (b2) displays this structure, even though the contrast is substantially weaker. This corroborates that

the here investigated Co/Pt and Co/Pd multilayers have a local multiloop memory that is facilitated by very small reverse domains that are substantially more stable toward annihilation in a positive field than toward expansion in a negative field. This asymmetric field dependence then causes a local domain expansion and retraction upon field cycling that enables a large macroscopic growth of the magnetization reversal amplitude in subsequent minor loop cycles, the phenomenon that we termed here cumulative minor loop growth.

While this effect is probably present in many magnetic materials, it appears to be particularly pronounced in perpendicular magnetized films of intermediate thickness. We did not observe this effect in very thin $[\text{Co/Pt}]_3$ multilayer³² and found only a much smaller effect in thicker $[\text{Co/Pd}]_{50}$ -multilayer samples. So, even though cumulative minor loop growth might be a more general phenomenon, it may be a rather small effect in most cases as it relies on the intricate nucleation-annihilation asymmetry discussed above.

ACKNOWLEDGMENTS

A.B. acknowledges funding from the Department of Industry, Trade, and Tourism of the Basque Government under Program No. IE06-172, the Department of Education, Universities, and Research of the Basque Government under Program No. PI2009-17, and the Provincial Council of Gipuzkoa, as well as from the Spanish Ministry of Science and Education under Projects No. CSD2006-53 and No. MAT2009-07980. J.M. thanks N. Martin for experimental help with the magneto-optical microscopy setup.

¹See, for instance, Giorgio Bertotti, *Hysteresis in Magnetism: For Physicists, Materials Scientists, and Engineers* (Academic Press, San Diego, 1998).

²It is hereby important to notice that H^* can be considerably smaller than the saturation field H_s due to thermal activation processes during magnetization reversal. See, for example, A. Berger, E. Marinero, M. Doerner, X. Bian, K. Tang, and A. Polcyn, *J. Appl. Phys.* **97**, 10N115 (2005).

³Y. L. He and G. C. Wang, *Phys. Rev. Lett.* **70**, 2336 (1993).

⁴J.-S. Suen and J. L. Erskine, *Phys. Rev. Lett.* **78**, 3567 (1997).

⁵See, for instance, R. S. Tebble and D. J. Craik, *Magnetic Materials* (Wiley-Interscience, London, 1969).

⁶X. Che and H. Suhl, *Phys. Rev. Lett.* **64**, 1670 (1990).

⁷E. Puppini, P. Vavassori, and L. Callegaro, *Rev. Sci. Instrum.* **71**, 1752 (2000).

⁸D. H. Kim, S. B. Choe, and S. C. Shin, *Phys. Rev. Lett.* **90**, 087203 (2003).

⁹M. S. Pierce, R. G. Moore, L. B. Sorensen, S. D. Kevan, O. Hellwig, E. E. Fullerton, and J. B. Kortright, *Phys. Rev. Lett.* **90**, 175502 (2003).

¹⁰M. S. Pierce, C. R. Buechler, L. B. Sorensen, J. J. Turner, S. D. Kevan, E. A. Jagla, J. M. Deutsch, T. Mai, O. Narayan, J. E. Davies, K. Liu, J. Hunter Dunn, K. M. Chesnel, J. B. Kortright, O. Hellwig, and E. E. Fullerton, *Phys. Rev. Lett.* **94**, 017202 (2005).

¹¹X. D. Liu, A. Berger, and M. Wuttig, *Phys. Rev. B* **63**, 144407

(2001).

¹²E. Della Torre and F. Vajda, *IEEE Trans. Magn.* **31**, 1775 (1995).

¹³V. G. Lewis, P. I. Mayo, and K. O'Grady, *J. Appl. Phys.* **73**, 6656 (1993).

¹⁴M. M. El-Hilo, A. L. Al-Momnee, and S. A. Bakar, *J. Appl. Phys.* **91**, 8742 (2002).

¹⁵J. Ferré, V. Grolier, P. Meyer, S. Lemerle, A. Maziewski, E. Stefanowicz, S. V. Tarasenko, V. V. Tarasenko, M. Kisielewski, and D. Renard, *Phys. Rev. B* **55**, 15092 (1997).

¹⁶I. D. Mayergoyz, *Phys. Rev. Lett.* **56**, 1518 (1986).

¹⁷I. Tagawa and Y. Nakamura, *IEEE Trans. Magn.* **27**, 4975 (1991).

¹⁸J. P. Sethna, K. Dahmen, S. Kartha, J. A. Krumhansl, B. W. Roberts, and J. D. Shore, *Phys. Rev. Lett.* **70**, 3347 (1993).

¹⁹R. J. M. van de Veerdonk, X. Wu, and D. Weller, *IEEE Trans. Magn.* **38**, 2450 (2002).

²⁰C. R. Pike, *Phys. Rev. B* **68**, 104424 (2003).

²¹A. Berger, Y. H. Xu, B. Lengsfeld, Y. Ikeda, and E. E. Fullerton, *IEEE Trans. Magn.* **41**, 3178 (2005); A. Berger, B. Lengsfeld, and Y. Ikeda, *J. Appl. Phys.* **99**, 08E705 (2006); Y. Liu, K. A. Dahmen, and A. Berger, *Appl. Phys. Lett.* **92**, 222503 (2008); A. Berger, N. Supper, Y. Ikeda, B. Lengsfeld, A. Moser, and E. E. Fullerton, *ibid.* **93**, 122502 (2008).

²²O. Hovorka, Y. Liu, K. A. Dahmen, and A. Berger, *Appl. Phys. Lett.* **95**, 192504 (2009); O. Hovorka, R. F. L. Evans, R. W.

- Chantrell, and A. Berger, *ibid.* **97**, 062504 (2010).
- ²³Y. L. Iunin, Y. P. Kabanov, V. I. Nikitenko, X. M. Cheng, D. Clarke, O. A. Tretiakov, O. Tchernyshyov, A. J. Shapiro, R. D. Shull, and C. L. Chien, *Phys. Rev. Lett.* **98**, 117204 (2007); Y. L. Iunin, Y. P. Kabanov, V. I. Nikitenko, X. M. Cheng, C. L. Chien, A. J. Shapiro, and R. D. Shull, *J. Magn. Magn. Mater.* **320**, 2044 (2008).
- ²⁴A. Pérez-Junquera, V. I. Marconi, A. B. Kolton, L. M. Álvarez-Prado, Y. Souche, A. Alija, M. Vélez, J. V. Anguita, J. M. Alameda, J. I. Martín, and J. M. R. Parrondo, *Phys. Rev. Lett.* **100**, 037203 (2008).
- ²⁵Our procedure is different from the sequence used by Ferré *et al.*, the only other study (Ref. 15), in which a clearly visible minor loop growth upon multiple field cycling was observed. Their procedure included an intermediate negative field pulse step for the purpose of generating a demagnetized state because their primary interest was the magnetization behavior of demagnetized states. As the focus of our study is the minor loop growth itself, we preferred to start our measurements from the saturated state to ensure repeatable starting conditions.
- ²⁶A. Lyberatos, *Comput. Mater. Sci.* **18**, 13 (2000).
- ²⁷M. Czapkiewicz, J. Kanak, T. Stobiecki, M. Kachel, M. Zoladz, I. Sveklo, A. Maziewski, and S. van Dijken, *Mater. Sci. (Poland)* **26**, 839 (2008).
- ²⁸R. Lavrijsen, G. Malinowski, J. H. Franken, J. T. Kohlhepp, H. J. M. Swagten, B. Koopmans, M. Czapkiewicz, and T. Stobiecki, *Appl. Phys. Lett.* **96**, 022501 (2010).
- ²⁹H. J. G. Draaisma and W. J. M. de Jonge, *J. Appl. Phys.* **62**, 3318 (1987); A. Berger and R. P. Erickson, *J. Magn. Magn. Mater.* **165**, 70 (1997); O. Hellwig, A. Berger, J. B. Kortright, and E. E. Fullerton, *ibid.* **319**, 13 (2007).
- ³⁰J. E. Davies, O. Hellwig, E. E. Fullerton, G. Denbeaux, J. B. Kortright, and K. Liu, *Phys. Rev. B* **70**, 224434 (2004); J. E. Davies, O. Hellwig, E. E. Fullerton, M. Winklhofer, R. D. Shull, and K. Liu, *Appl. Phys. Lett.* **95**, 022505 (2009).
- ³¹X. M. Cheng, V. I. Nikitenko, A. J. Shapiro, R. D. Shull, and C. L. Chien, *J. Appl. Phys.* **99**, 08C905 (2006).
- ³²D. T. Robb, Y. H. Xu, O. Hellwig, J. McCord, A. Berger, M. A. Novotny, and P. A. Rikvold, *Phys. Rev. B* **78**, 134422 (2008).